Available online www.jocpr.com

Journal of Chemical and Pharmaceutical Research, 2017, 9(12):164-173

Research Article

ISSN : 0975-7384
CODEN(USA) : JCPRC5

Synthesis, Characterization, Biological and Anticancer Activity of New Pd(II), Pt(IV),V(III) and Ru(III) Complexes with a Schiff Base Ligand Deriving from Dehydroacetic Acid

Tahani I Kashar*

Faculty of Arts and Science, Department of Chemistry, Qassim University, Buraydah, Saudia Arabia

---

ABSTRACT

The solid complexes of Pd(II),Pt(IV),V(III) and Ru(III) with Schiff base ligand(HL) derived from heterocyclic compounds 3-acetyl-6- methyl-(2H)-pyran-2,4(3H)-dione (Dehydroacetic acid) and 4-aminoantipyrine were synthesized and characterized by elemental analysis,IR,1H-NMR, molar conductance, magnetic moment, UV-Vis and thermal analysis (TG/DTG). The magnetic moment and spectral data suggest that the V(III)and Ru(III) complexes have octahedral geometry while the Pd(II)and Pt(IV) complexes have square planar geometry. The ligand coordinated to the metal ions as tridentate, with ONO donor sites. The thermal behavior of these complexes shows that the complexes loose of lattice and or coordination water molecules in the first step and is followed by decomposition of the anions and ligand moieties in the respective steps. The ligand and their metal complexes were also screened for their antibacterial activity against bacterial species as well as fungi. The activity data show that the metal complexes to be more potent antimicrobial than the parent ligand. The antibacterial activity follow the order:HL<V(III)<Ru(III)<Pd(II) =Pt(IV)for G- bacteria Escherichia coli and HL<V(III)<Ru(III)=Pt(II)<Pd(II)for G+ bacteria Staphylococcus aureus. The Pd(II) complex has antifungus effect against aspergillus flavus while the ligand (HL) and V(III) complex has antifungus effect against Candida albicans. The IC50 values toward human liver cancer cell lines HEPG2 takes the following order HL<V(III)<Pd(II)<Pt(II)<Ru(III) and that for human breast cell lines MCF7 takes the following orderV(III)<Pt(IV)<Pd(II)<HL<Ru(III).

Keywords: Synthesis; DHA; Metal complexes; Antibacterial; Antifungi; Anticancer effect

---

INTRODUCTION

Dehydroacetic acid (DHA = 3-acetyl-4-hydroxy-6-methyl-*2H*-pyran-2-one), and their derivatives are very important class of compounds for various organic synthesis [1]. It is a good starting material for the synthesis of different heterocyclic compounds [2]. Dehydroacetic acid (DHA) is biologically active compound and studies have shown that it has both antibiotic and antifungal effects [3]. It is a very strong antiseptic agent [4]. The dehydroacetic acid compounds were used to increase the stability of vitamin C and to protect vegetables during processing of food [5] and as preservatives in fish sausages [6]. In view, its Schiff base and their complexes have a high degree of activities. On the other side antipyrine and its derivatives have wide applications in biological activities [7,8]. Schiff bases of 4-aminoantipyrine and their complexes have a variety of applications in biological, clinical, analytical, and pharmacological areas [9-13]. 4-Aminoantipyrine derivatives are very important in the field of coordination complexes and also these compounds are reported to exhibit analgesic and anti-inflammatory effects, antiviral, antibacterial, anti-cancer and herbicidal activities[14-19]. All these reasons made me interested to synthesize and structurally characterize the Schiff base of dehydroacetic acid with 4-aminoantypyrine and their Pd(II), Pt(II), V(III) and Ru(III) complexes and also to check the biological activities of these compounds. So, in the present study the Schiff base were synthesized by the reaction of dehydroacetic acid with 4-aminoantipyrine and their Pd(II), Pt(II),

V(III) and Ru(III) complexes were prepared and characterized by molar conductance, magnetic susceptibility measurements, ultra-violet, infrared spectroscopy and thermal analyses (TG, DTG)studies. Their antibacterial activities were evaluated by measuring the zone of inhibition using disc diffusion method against Gram positive bacteria *Staphylococcus aureus*, and gram negative bacteria *Escherichia coli*. The cytotoxicity of the ligand (H_2L) and its Pd(II), Pt(II), V(III) and Ru(III) complexes on human liver HEPG2 and on breast MCF7 carcinoma cells lines were determined and the results of the cytotoxic activity *in vitro* were expressed as IC50 values.

EXPERIMENTAL SECTION

Measurements

All chemicals and solvents used were pure chemicals from BDH or Aldrich and used as received. Melting points are in degree centigrade and are uncorrected. Infrared spectra were recorded on a Mattson – 5000 FTIR spectrometer using potassium bromide and ^{1}H-NMR spectra were determined on a Varian Gemini – 200 MHz, jeol–Ex–250 MHz NMR spectrometer in DMSO solvent and TMS as an internal standard with (chemical shift. δ=0 ppm), Faculty of Science, Cairo University, Mass spectra were determined on a GC-MS. Qp–1000 Ex (Shimadzu, Japan), faculty of science, Cairo University. The purity of the synthesized compounds was tested by thin layer chromatography (TLC), Merck plates. Elemental analyses (C, H, N and Cl) were carried out at the micro analytical Unit of the University of Cairo. Metal ions were determined using atomic absorption with a Perkin Elmer (model 2380) spectrophotometer. Electronic absorption spectra in the 200-900 nm regions were recorded on a Perkin-Elmer 550 spectrophotometer. Thermal analyses (TG and DTG) were carried out on a Shimadzu DT-30 and TG-50 thermal analyzers in the 27-1000°C range at a heating rate of 10°C min^{-1}. The magnetic susceptibilities were measured at room temperature using the Gouy method with mercuric tetrathiocyanatocobaltate(II) as magnetic susceptibility standard; diamagnetic corrections were made using Pascal's constants. A Bibby conductimeter MCl was used for conductance measurements.

Synthesis of the Ligand

A mixture of (50 ml) ethanolic solution of dehydroacetic acid (DHA) (0.01 mol) and 4-aminoantypyrine (0.01 mol) was mixed. The mixture was refluxed for 5h, concentrated and cooled. The pale yellow precipitate which formed was filtered off, dried and recrystallization from ethanol M.p:210˚C, yield 90%. Elemental analysis: (Found C=64.0%, H=5.6%, N=11.2%). $C_{19}H_{19}N_3O_4$ (calculated: C=64.5%, H=5.4%, N=11.9%. IR (KBr):ν3434, 1706, 1663 and 1563 cm^{-1} of (OH), ($C=O_{DHA}$), ($C=O_{antipyrine}$) and (C=N) groups respectively. MS [m/z] (%): 353 [M^+], 269, 234, 212, 203, 151, 137, 109, 83 and 56.

Synthesis of the Complexes

The hot ethanolic solutions of corresponding metal chloride, Pd(II), Pt(II), V(III) and Ru(III) (0.05 mol) salts and the ligand (0.05 mol) were mixed and refluxed for about 3-5 hours to get the metal complexes. The refluxed solution was cooled for overnight and filtered. The obtained metal complexes dried in desiccators over anhydrous calcium chloride.

[LPdCl] $2H_2O$ complex:

Deep brown ppt. was formed with yield 85% M.p: 260°C. Elemental analysis: (Found: C= 43.0%, H= 3.8%, N =8.6%, Pd= 19.8% and Cl=6.9). [Pd ($C_{19}H_{18}N_3O_4$)Cl]$2H_2O$ (Calculated: C=43.0%, H =4.1%, N =7.9%, Pd =20% and Cl =6.7%.IR(KBr): ν3432, 1697, 1670 and 1556cm^{-1}of (OH_{water}), ($C=O_{DHA}$), ($C=O_{antipyrine}$) and (C=N) groups and at 539,470and440cm^{-1} of Pd-N, Pd-N and Pd-Cl bonds respectively.

[LPtCl]$Cl_2.2H_2O$ complex:

Deep brown ppt. was formed with yield 80% M.p: 270°C. Elemental analysis: (Found: C=32.6%, H=3.1%, N=6.3%, Pt=28.0% and Cl=15.0% Pt ($C_{19}H_{18}N_3O_4$)Cl_3. $2H_2O$(Calculated: C=33.0%, H=3.2%, N=6.1%, Pt=28.2% and Cl=15.4%. IR (KBr): ν3433, 1690, 1600, 1550, cm^{-1} of (OH_{water}), ($C=O_{DHA}$), ($C=O_{antipyrine}$) and (C=N) groups and at 540, 499 and 460 of Pt-O, Pt-N and Pt-Cl bonds respectively.

[L $VCl_2.H_2O$] complex:

Pale brown ppt. was formed with yield 85% M.p: >300°C. Elemental analysis: (Found: C=46.4%, H=3.7%, N=8.0%, V=10.3% and Cl=14.0% [V ($C_{19}H_{18}N_3O_4$)$Cl_2.H_2O$] (calculated: C=46.2%, H=4.1%, N=8.5%, V=10.0% and Cl=14.4%. IR (KBr): ν3430, 1650, 1728 and 1564 cm^{-1} of (OH_{water}), ($C=O_{DHA}$), ($C=O_{antipyrine}$) and (C=N) groups and at 545, 490 and 460 cm^{-1} of V-O, V-N and V-Cl bonds respectively.

[LRuCl $(H_2O)_2$]Cl.6H_2O complex:
Black ppt. was formed with yield 80% M.p: >300˚CElemental analysis: (Found: C=32.6%, H=3.1%, N=6.3%, Ru=15.2% and Cl=10.8% Ru ($C_{19}H_{18}N_3O_4$)Cl_2.8H_2O (Calculated: C=33.0%, H=3.2%, N=6.1%, Ru=15.1% and Cl=10.6%. IR (KBr): ν3430, 1600 and 1555 cm^{-1} of (OH_{water}), ($C=O_{DHA}$), ($C=O_{antipyrine}$) and (C=N) groups and at 510, 470 and 430 cm^{-1} of Ru-O, Ru-N and Ru-Cl bonds respectively.

Table 1: IR spectra of of the ligand and their complexes

No.	Molecular Formula	OHν	C=O(DHA)ν	C=Oν (4-NH_2antypyrine	νC=N	M-Oν	M-Nν	Λοημ–^{1}χμ^{2}μολ^{-1}
1	HL($C_{19}H_{19}N_3O_4$)	3434(br.)	1706(s)	1663(s)	1563(s)	-	-	15
2	[LRuCl $(H_2O)_2$]Cl.6H_2O	3430(br.)	-	1600(s)	1555(s)	510(s)	470(w)	90
3	[LPdCl]2H_2O	3432(br.)	1697(s)	1630(s)	1556(s)	539(m)	470(w)	30
4	[LPtCl]Cl_2.2H_2O	3433(br.)	1690(m)	1600(m)	1550(s)	540(w)	499(w)	160
5	[L VCl_2.H_2O]	3430(br.)	1728(s)	1650(s)	1562(s)	545(s)	490(w)	20

Antimicrobial Activity
The ligand and their metal complexes were evaluated for their *in vitro* antibacterial activity against *Escherichia coli*, *Staphylococcus aureus* and antifungal activity against *Aspergillus flavus* and *Candida albicans* using a modified Kirby- Bauer disc diffusion method [20]. Plates inoculater with filamentous fungi as *Aspergillus flavus* at 25°C for 48 hours; Gram + bacteria as *Staphylococcus aureus*; Gram – bacteria as *Escherichia coli* they were incubated at 35-37°C for 24-48 hours and yeast as *Candida albicans* incubated at 30°C for 24-48 hours and then the diameters of the inhibition zones were measured in millimeters. Standard discs of Ampicillin (Antibacterial agent) and Amphotericin B(Antifungal agent) served as positive controls for antimicrobial activity but filter discs impregnated with 10 µl of solvent DMSO were used as negative control. For the disc diffusion the zone diameters were measured with slipping calipers of the National Committee for Clinical Laboratory Standards [21]

Cytotoxic Activity
The cytotoxicity of the compounds was tested at the National Cancer Institute, Cairo University Egypt by SRB assay using the method of Suresh et al. cells were plated in 96-multiwell plate (10^4 cells/well) for 24 h before treatment with the compounds to allow attachment of cell to the wall of the plate. Different concentrations of the compound under test (5, 12, 25 and 50 µg/ml) were added to the cell monolayer triplicate wells were prepared for each individual dose. Monolayer cells were incubated with the compounds for 48 h at 37ºC and in atmosphere of 5% CO_2. After 48 h, cells were fixed, washed and stained with Sulfo- Rhoda-mine-B stain. Excess stain was washed with acetic acid and attached stain was recovered with Tris EDTA buffer. Color intensity was measured in an ELISA reader. The relation between surviving fraction and drug concentration is plotted to get the survival curve of each tumor cell line after the specified compound [22].

RESULTS AND DISCUSSION

In this paper, new Schiff base derived from dehydroacetic acid and 4-aminoantypyrineand their metal complexes of Pd(II), Pt(II), V(III) and Ru(III) were prepared and characterized. The metal complexes are stable in air and insoluble in most common organic solvents, freely soluble in DMF/ DMSO, non-hygroscopic in nature and colored. The structure of the synthesized compounds was established by the various spectroscopic techniques. The results of elemental analyses (C, H, N and Cl) and melting points confirmed the proposed molecular formula of the complexes. The conductance of the ligand and all the synthesized metal complexes were recorded in 10^{-4} M DMF at room temperature, the molar conductance values indicated that the complexes[LPtCl]Cl_2. 2H_2O and [LRuCl $(H_2O)_2$]Cl. 6H_2O are conductance. The results obtained are in good agreement with those calculated for the suggested formulae.

Mass Spectra
The mass spectra of free ligand (Figure 1) displayed an intense molecular cation peak at *m/z* 353.0 due to (M^{+1}). The observed value was corresponds to the molecular weight of the ligand under investigation. Other prominent peaks in the mass spectrum were observed at *m/z* 269, 234, 212, 203, 151, 137, 109, 83 and 56. These observed *m/z* peaks were due to the loss of the fragments of different molecular weights from ligand as proposed in Scheme 1.

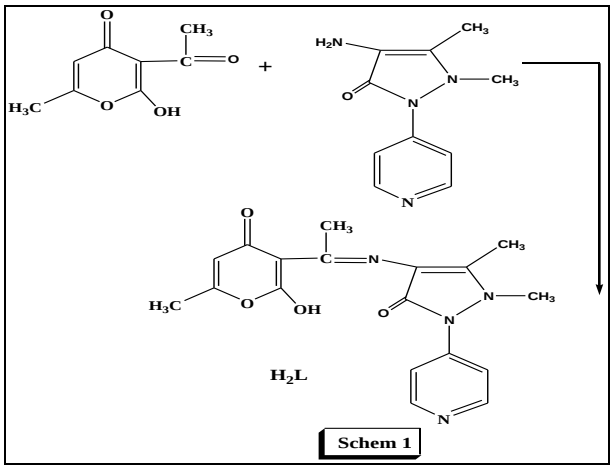

Scheme 1: Mass spectra of the ligand (HL)

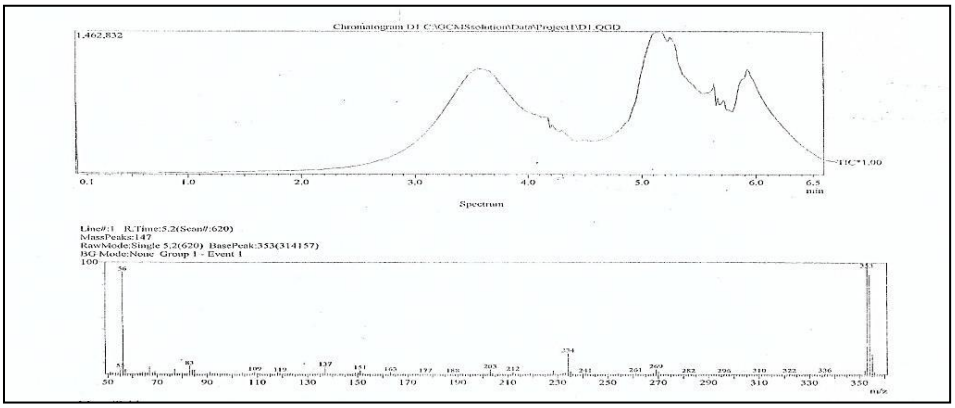

Figure 1: Mass spectra of the ligand (HL)

H[13]C NMR Spectra

The ^{1}H NMR spectrum of the ligand showed signals at 2.12 ppm as a singlet due to methyl protons of DHA ring, 2.65 ppm due to N=C-CH_3 (singlet), 6.87-7.81 ppm (multiplet) due to aromatic protons and the signals due to the protons of pyridine ring appeared at 6.6-8.4 ppm, 5.77 ppm (singlet) due to olefinic proton. The signal due to enolic proton was observed at 15.99 ppm. In ^{13}C NMR of ligand the aromatic carbons resonated at δ 121.63-161.41. The methyl carbons resonated at 16.89 and 19.29 ppm. DHA ring carbons showed chemical shifts at 161.41, 106.19, 94.76 and 171.02 ppm, respectively.

IR Spectra

IR spectrum of free ligand displayed the characteristic bands at 3434 cm^{-1}, 1706 cm^{-1}, 1663 cm^{-1} and 1563 cm^{-1}, these bands were assigned to υOH (intramolecular hydrogen bonding), υ C=O ((lactone carbonyl), C=O(4-aminoantypyrine) and C=N(azomethine) groups respectively [23] (Figure 2). The C=N(azomethine) stretching frequencies showed downward shift in all the metal complexes which suggested the involvement of this N atom in coordination [24]. The band corresponding to C=O at 1663 cm^{-1} of antipyrine was shifted to lower frequency in the metal complexes, suggesting the coordination to the metal ions [25] (Table 1). Theses drastic change in the υ(C=O) stretching frequencies which suggested that the ligand is coordinated with the metal ions through carbonyl oxygen atom C=O(4-aminoantypyrine) [25]. The disappearance of phenolic oxygen stretching frequency in the region 1360-1375 cm^{-1} in all the metal complexes compared to the ligand indicates the coordination of phenolic oxygen atom via deprotonation [26]. The broad bands at 3400-3330 cm^{-1} were assigned to crystallized or coordinated water molecules in complexes [23]. The IR spectra of the complexes showed new bands in the 545–510, 502–450 and 460-430 cm^{-1} regions, which can be assigned to (M–O), (M–N) and (M-Cl) vibrations, respectively [27,28].

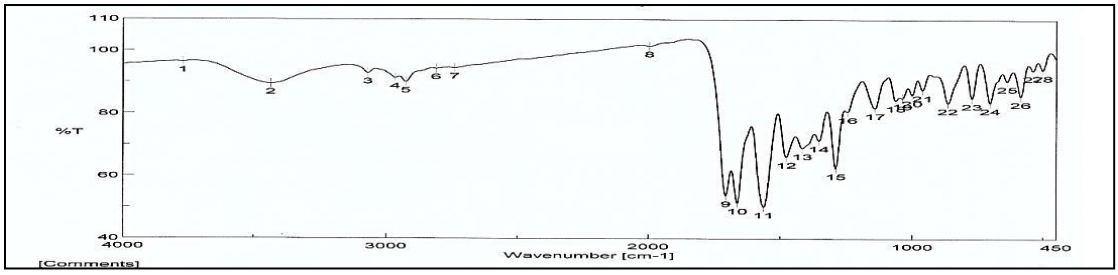

Figure 2: IR spectrum of the ligand (HL)

UV-Vis Spectra and Magnetic Moment

The electronic spectra of the DMF solutions of the ligand exhibit bands in the range 292-320 nm assigned to the π → π* and n→ π* transitions, of the azomethine C=N and C=O moieties, and it is shifted to longer wavelength on coordination through azomethine nitrogen in the complexes (Table 2). In all complexes charge transition spectra occurred at 360-422nm [29]. In Ru(III) and V(III) complexes the bands at 520- 500 nm due to $2T_{2g}\rightarrow 4T_{2g}$ and $2T_{2g}\rightarrow 2A_{2g}$, $2T_{1g}$ transitions of low spin octahedral geometry. The magnetic moment values observed for the Ru(III) complexes is 2.3 BM that correspond to the presence of one unpaired electron, indicating the low-spin nature of the complex. The V(III) complex show magnetic moment 2.9 BM consistent with a d^2 electronic configuration this indicated that the Ru(III) and V(III) complexes have octahedral structure. The room temperature magnetic moments values of the Pd(II) and Pt(IV) complexes show that are diamagnetic.

TG and DTG Thermal Analyses

The data obtained aggrement with the proposed structure of the prepared complexes **(**and indicate that Ru(III) complex undergo five steps degradation reaction (Table 2), the first step occur at T_{max}81.63°C, the weight loss 5.38% associated with this step agrees quite well with the loss of two lattice water molecule, the second step occur at T_{max} 244.80ºC with weight loss 26.76% it referred to loss of 6 $H_2O$and Cl_2, and the third decomposition step due to loss of Pyridine and $2CH_3$ with weight loss 16.30%. The fourth step referred to loss of CO_2 and CH_3 and the further fifth decomposition due to loss of NH_3 and CH_3 weight losses 8.8 and 4.78% respectively. The residual is in agreement with Ru_2O_3. The thermal decomposition of Pd(II) complex may be characterized as a four decomposition steps with weight losses 13.47, 23.36, 14.3 and 4.9% respectively, the first step at T_{max} 226.62ºC is due to loss of two lattice water and HCl, the second step appeared at T_{max} 280.58 due to loss of $3CH_3$ and Pyridine ring, the third decomposition occurs at T_{max} 316.01 due to loss of CO_2, NH_3 and CH_3.

Table 2: UV spectral data and (TG, DTG) thermal analyses of the ligand and their complexes

No.	Compounds	UV Spectra λ_{max}(nm)			TG Peaks		DTG Peaks	
		n-π*	π-π*	C-T	Temp.°C	wt lost %(calc.)found	Temp.°C	Assignment
1	$HL(C_{19}H_{19}N_3O_4)$	3,20,302	292	-	178.6-731.4	81.5	202.65 289.73	Thermal decomposition
2	$[LRuCl(H_2O)_2]Cl.6H_2O$	3,18,300	296	36,44,40,510	43.29-162.99	(5.38)4.68	81.63	Loss of two lattice water
					162.99-362.32	(26.76)27.13	244.8	Loss of 6 H_2O+Cl_2
					362.32-518.88	(16.30)17.21	295.26	Loss of Py+$2CH_3$
					518.88-646.31	(8.8)7.9	459.29	Loss of CO_2+CH_3
					646.31-1001.74	(4.78)5.29	527.93	Loss of NH_3+CH_3
3	$[LPdCl]2H_2O$	3,20,314	300	3,88,376	49-83-257.76	(13.47)13.26	226.62	Loss of two lattice water + HCl
					257.76-317.87	(23.36)22.88	280.58	Loss of $3CH_3$+Py
					317.87-447.6	(14.3)13.3	316.01	Loss of CO_2+NH_3+CH_3
					447.6-648.7	4.9	863.2	Thermal decomposition
4	$[LPtCl]Cl_2.2H_2O$	330	296	3,80,370	59.54-175.86	(12.88)12.62	119.01	Loss of H_2O+Cl_2
					175.86-312.32	(20.60) 19.23	166.27	Loss of H_2O+HCl
					312.32-1000.4	(22.14)23.14	288.72	Loss of $2CH_3$ +CO_2 +Py
5	$[L\ VCl_2.H_2O]$	310	300	36,04,10,510	43.62-268	(3.64)3.12	240	Loss of one coordinate water
					268.8-368.9	(20.47)20.38	350	Loss of $2CH_3$ +Cl_2
					368.91-555.9	(22.09)23.40	520	Loss of $2CH_3$ +Py
					555.9-1000.4	(11.96)12.7	980	Loss of CO_2+NH_3

The residual is in agreement with $PdCO_3$. For the pt(IV) complex the first mass loss is due to losses of H_2O and Cl_2 and occurs from 59.54-175.86°C with weight losses 12.88%, the second decomposition at175.86-312.32ºC due to

loss of H_2O and HCl with weight losses 20.60%, the third step occurs at 312.32-1000.4°C with weight losses 22.14% due to losses of $2CH_3$,CO_2 and Pyridine ring. The residual is in agreement with $Pt(CO_3)_2$. The thermal decomposition of V(III) complex occurs in fourth steps, the first at 43.62-268°C with weight loss 3.64 due to loss of one coordinated water, the second step appeared at 268.8-368.9°C due to loss of $2CH_3$ and Cl_2 weight loss 20.47%, the third step at 368.91-555.9 due to loss of $2CH_3$ and Pyridine with weight loss 22.09%, the last step occurs at 555.9-1000.4 with weight loss 11.96% due to thermal decomposition of NH_3 and CO_2. The residual is in agreement with V_2O_5 (Figure 3).

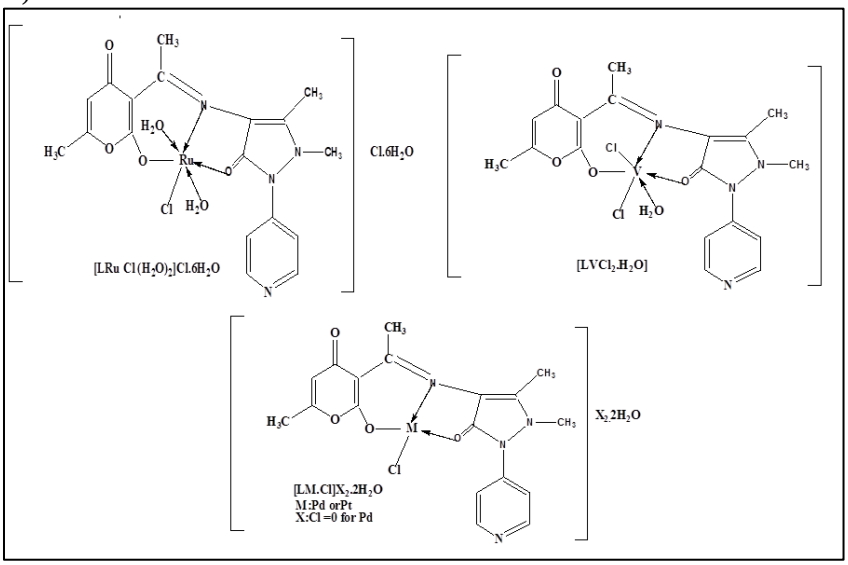

Figure 3: The structure of the complexes of the ligand (HL)

Biological Activity

The ligand and their Pd(II), Pt(II), V(III) and Ru(III) complexes exhibited varying degrees of inhibitory effects on the growth of the tested bacterial species *Escherichia coli*, *Staphylococcus aureus* and for antifungal activity against *Aspergillus flavus* and *Candida albicans* (Table 3). Ampicillin trihydrate for bacteria and Amphotericin B for fungi were used as reference drugs. The ligand is moderately active against the bacterial species while the complexes are more active [30,31]. Referring to complexes, we note that the Pd(II) complex is more antibacterial activity as compared with other complexes [32]. In conclusion, the antibacterial activity follow the order: HL<V(III)<Ru(III)<Pd(II) = Pt(IV)for G- bacteria *Escherichia coli* and HL<V(III)<Ru(III) = Pt(II) <Pd(II)for G+ bacteria *Staphylococcus aureus* (Figure 4). The Pd(II) complex has antifungal effect against *aspergillus flavus* while the ligand and V(III) complex has antifungal effect against *Candida albicans*. Generally the Pd(II) complex can be used for the treatment of some common diseases caused by *Escherichia coli*, *Staphylococcus aureus* and *aspergillus flavus*. An antibacterial activity of metal complexes better than the ligand can be explained on the basis of Overtone's and Tweedy's concepts [33]. Upon chelation, the positive charge of the metal ion is partially shared with the donor atom present on the ligand and a π -electron delocalization over the whole chelate ring takes place. In this way, the lipophilic character of the metal chelate increases and favours its permeation through the lipoid layers of the bacterial membranes and blocks the metal binding sites in the microorganism. Thus the compounds reported may possess a possible antitumor effect.

Table 3: Biological activities of the ligand and their metal complexes against some microbial pathogens

Treatments DMSO	Inhibition zone diameter (mm / mg of complex)			
	Esherishia coli (G-)	*Staphylococcus aureus (G+)*	*Aspergillusflavus (Fungus)*	*Candida albicans (Yeast)*
Negative Control	0	0	0	0
Ampicillin (Antibacterial agent)	22	18	0	0
Amphotericin B (Antifungal agent)	0	0	17	19
HL (Ligand)	9	9	0	15
$[LRuCl(H_2O)_2]Cl.6H_2O$	12	13	0	0
$[LPdCl]2H_2O$	13	14	11	0
$[LPtCl]Cl_2.2H_2O$	13	13	0	0
$[L\ VCl_2.H_2O]$	11	11	0	11

DMSO: dimethylsulfoxidesolvent; G^- : Gram negative bacteria; G^+: gram positive bacteria

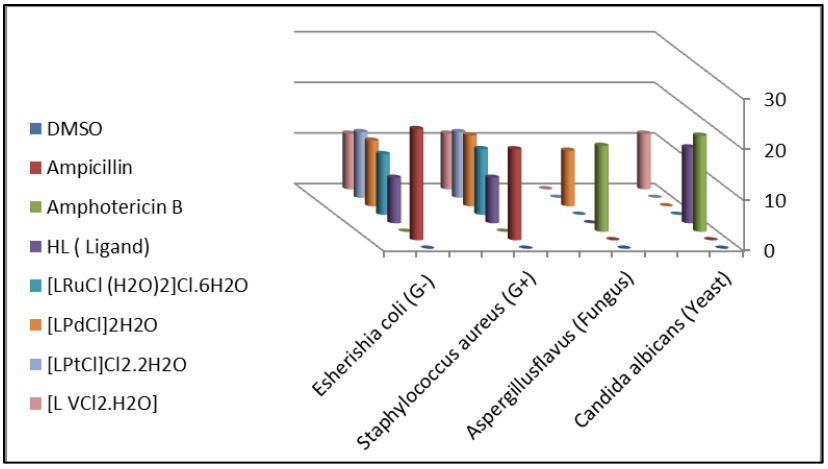

Figure 4: Inhibitory zone of the ligand and their complexes against some kind of bacteria (+/-) and fungi

Cytotoxic Activity

In the present study the antitumor activity of the ligand and their Pd(II), Pt(II), V(III) and Ru(III) complexes were evaluated (Tables 4 and 5). The half maximum inhibitory concentrations (IC_{50}) of the ligand and their complexes against breast and liver carcinoma cells HEPG2 and MCF7 *in vitro* by ELISA methods were detected by using four serial concentrations (5, 12, 25 and 50 µg/ml). The results of the cytotoxic activity were expressed as IC_{50} (the concentration of the compound in ug/ml that inhibits proliferation of the cells by 50% as compared to the untreated control cells) are given in Tables 4 and 5. The IC50 value toward human liver cancer cell lines HEPG2 takes the following order HL<V(III)<Pd(II)<Pt(II)<Ru(III) (Figures 5 and 6) and that for human breast cell lines MCF-7 takes the following order V(III)<Pt(IV)<Pd(II)<HL<Ru(III) (Figures 7 and 8). We can concluded that the ligand and V(III) complexes have a significant antitumor activity against breast carcinoma cells (MCF-7 cell line) but V(III) and Pt(IV) have a significant antitumor activity against liver carcinoma cells (HEPG2cell line). The disscuction may be due to the action of these complexes involves binding to DNA and RNA of carcinoma cell and antitumor activity of tested complexes increase with its concentrations [34,35]. These results agrees with the above results [32,36].

Table 4: Antitumor data of the ligand (HL) and their Ru(III), Pd(III), Pt(III) and V(III) complexes against liver HEPG2 cells

Conc.: ug/ml	0	5	12.5	25	50	IC50 µg/ml
HL(C19H19N3O4)	1	0.912	0.689	0.481	0.435	23.7
$[LRuCl(H_2O)_2]Cl.6H_2O$	1	0.894	0.625	0.594	0.455	41.7
$[LPdCl]2H_2O$	1	0.751	0.717	0.544	0.426	34.7
$[LPtCl]Cl_2.2H_2O$	1	0.897	0.648	0.53	0.453	34.8
$[L\ VCl_2.H_2O]$	1	0.843	0.65	0.495	0.352	24.6

Table 5: Antitumor data of the ligand (HL) and its Ru(III), Pd(III), Pt(III)and V(III) complexes against breast MCF7 cells

Conc.: ug/ml	0	2.5	5	25	50	IC50 µg/ml
$HL(C_{19}H_{19}N_3O_4)$	1	0.941	0.707	0.439	0.318	20.5
$[LRuCl(H_2O)_2]Cl.6H_2O$	1	0.887	0.695	0.544	0.318	30
$[LPdCl]2H_2O$	1	0.917	0.708	0.435	0.287	20.2
$[LPtCl]Cl_2.2H_2O$	1	0.983	0.854	0.347	0.389	18.8
$[L\ VCl_2.H_2O]$	1	0.741	0.636	0.393	0.253	16.7

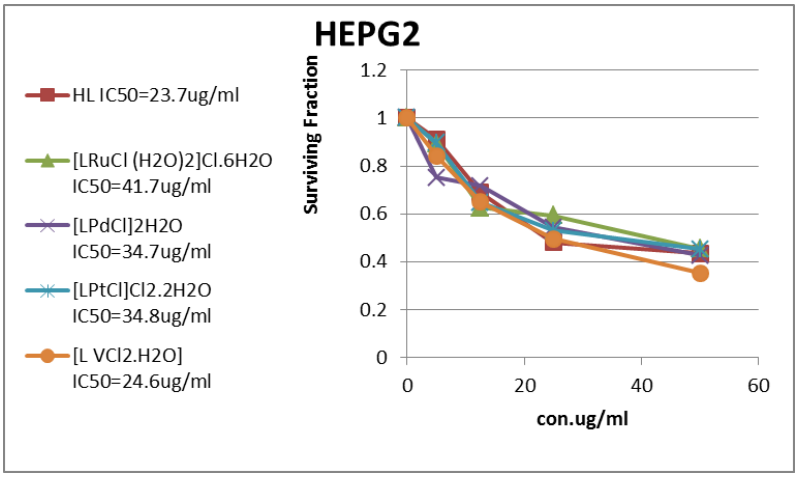

Figure 5: Antitumor test of the ligand (HL) and its Ru(III), Pd(III), Pt(III) and V(III) complexes against liver HEPG2 cells

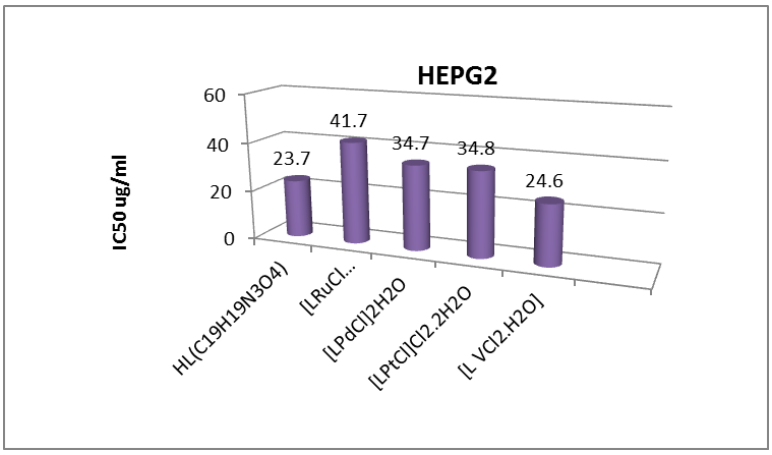

Figure 6: IC50 µg/ml values of the ligand(HL) and its Ru(III), Pd(III), Pt(III) and V(III) complexes against liver HEPG2 cells

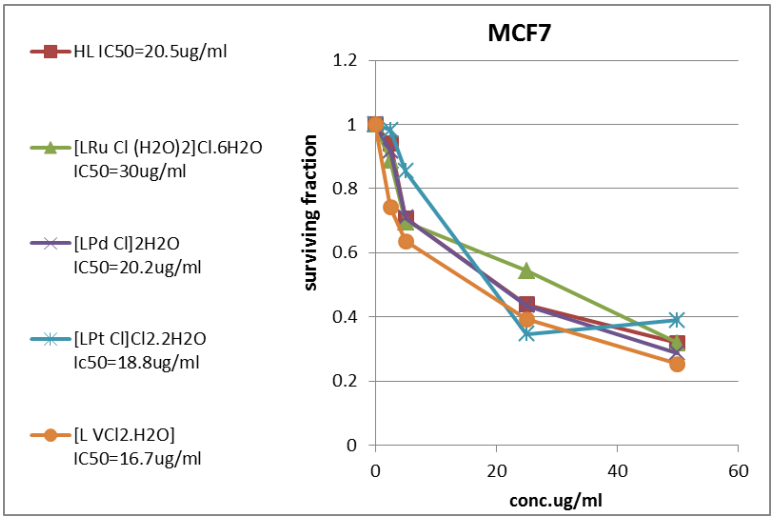

Figure 7: Antitumor test of the ligand (HL) and its Ru(III), Pd(III), Pt(III) and V(III) complexes against breast MCF7 cells

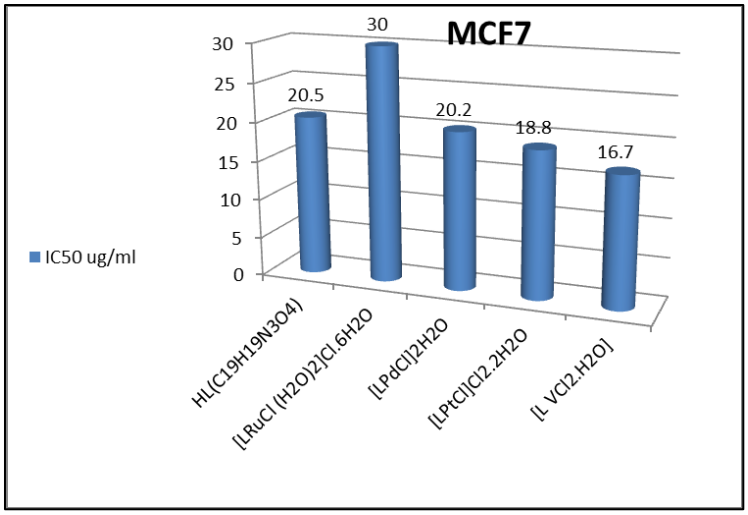

Figure 8: IC50 µg/ml valus of the ligand (HL) and its Ru(III), Pd(III), Pt(III) and V(III) complexes against breast MCF7cells

CONCLUSION

New Pd(II), Pt(II), V(III) and Ru(III) complexes with the Schiff base ligands derived from dehydroaceticacid and 4-aminoantipyrine were synthesized and characterized by spectral analysis. Coordination of the Schiff base to the metal atom was found to be through ONO doner sites as tridentate. The geometry of the complexes is assigned as square planar for Pd(II) and Pt(IV) complexes and as octahedral for Ru(III) and V(III) complexes. The antimicrobial studies reveal that the complexes show higher activity than the ligand. The antibacterial activity follow the order: HL<V(III)<Ru(III)<Pd(II)=Pt(IV)for G- bacteria *Escherichia coli* and HL<V(III)<Ru(III)=Pt(II)<Pd(II)for G+ bacteria *Staphylococcus aureus*. The Pd(II) complex has antifungus effect against *Aspergillus flavus* while the ligand (HL) and V(III) complex has antifungal effect against *Candida albicans*. The IC50 values toward human liver cancer cell lines HEPG2 takes the following order HL< V(III)<Pd(II)<Pt(II)<Ru(III) and that for human breast cell lines MCF7 takes the following order V(III)<Pt(IV)<Pd(II)<HL<Ru(III).

ACKNOWLEDGMENT

The author gratefully acknowledges Qassim University, represented by the Deanship of Scientific Research, on the material support for this research under the number **(**3102) during the academic year 1437 AH/2016AD.

REFERENCES

[1] M Cindric; V Vrdoljak; TK Novak; M C´uric; A Brbot-Saranovic; Kamenar. *J Molec Struc*. **2004**, 701, 111-118.
[2] Z Guo; G Faraglia; S Sitran. *Trans Met Chem*. **1995**, 20, 91-96.
[3] J Iqbal; FH Wattoo; SA Tirmizi; MHS Wattoo. *J Chem Soc Pak*. **2007**, 29,136-139.
[4] AL Kubaisi; K Ismail. *Can J Chem*. **1994**, 72, 1785-1788.
[5] CA Benassi; A Bettero; P Manzini; A Semenzato; P Traldi. *J Soc Cosmet Chem*. **1988**, 39, 85-92.
[6] AS Al Alousi; MR Shehata; MM Shoukry; SA Hassan; N Mahmoud. *J Coord Chem*. **2008**, 61, 1906-1916.
[7] KZ Ismail; A El-Dissouky; AZ Shehada. *Polyhedron*. **2009**, 16, 2909.
[8] AM Farghaly; A Hozza. *Pharmazie*. **1980**, 35, 596.
[9] YY Liu; H Wang; F Li. *J Mol*. **2013**, 18, 893.
[10] T Rosu; S Pasculescu; V Lazar; C Chifiriuc; R Cernat. *Molecules*. **2006**, 11, 914.
[11] G Turhan-Zitouni; M Sivaci; FS Kilic; K Erol. *Eur J Med Chem*. **2001**, 36, 689.
[12] T Hitoshi; N Tamao; A Hideyuki; F Manabu; M Takayuki. *Polyhedron*. **1997**, 16, 3787-3797.
[13] T Punniyamurthy; SJS Kalra; J Iqbal. *Tetrahedron Lett*. **1995**, 36, 8497-8712.
[14] CH Sayed; AA Hamed; GA Meligi; WE Boraie; M Shafik. *Molecules*. **2003**, 8, 322-332.
[15] Y Peng; H Zhong; ZF Chen; YC Liu; GH Zhang; QP Qin; H Liang. *Chem Pharm Bull*. **2014**, 62, 221-228.
[16] G Turan-Zitouni; M Sivaci; FS Kilic; K Erol. *Eur J Med Chem*. **2001**, 36, 685-689.

[17] SM Sondhi; VK Sharma; N Singhal; RP Verma; R Shukla; R Ranghubir; MP Dubey. *J Phosphorus Sulfur Silicon Relat Elem*. **2000**, 156, 21-33.
[18] D Burdulene; A Palaima; Z Stumbryavichyute; Z Talaikite. *Pharm Chem J*. **1999**, 33, 191-193.
[19] AZ El-Sonbati; MA Diab; AA El-Bindary; MK Abd El-Kader. *Spectrochim Acta A*. **2012**, 99, 211-217.
[20] AW Bauer; WM Kirby; C Sherris; M Turck. *Am J Clin Path*. **1966**, 45, 493-496.
[21] National Committee for Clinical Laboratory Standards. Methods for dilution antimicrobial susceptibility tests for bacteria that grow aerobically. 4th edition Approved standard M 7-A4. Wayne, Pa: National Committee for Clinical Laboratory Standards, **1997**.
[22] PK Suresh; MR Vijaybabu; A Arunkumar; J Arunakaranl. *J Ethnopharmacol*. **2006**, 105, 246-250.
[23] K Nakamoto. Infrared and Raman Spectra of Inorganic and Coordination Compound. Wiley, New York, **1978**.
[24] M Wang; LF Wang; YZ Li; QX Li; ZD Xu; DM Qu. *Trans Met Chem*. **2001**, 26, 310.
[25] S Chandra; S Raizada; M Tyagi; A Gautam. *Bioinorg Chem Appl J*. **2007**.
[26] AD Kulkarni; GB Bagihalli; SA Patil; PS Badami. *J Coord Chem*. **2009**, 62, 3072.
[27] R Natrajan; K Antonysamy; C Thangaraja. *Transition Met Chem*. **2003**, 28, 29.
[28] GB Bagihalli; PG Avaji; SA Patil; PS Badami. *Eur J Med Chem*. **2008**, 43, 2649.
[29] ABP Lever, Inorganic Electronic Spectroscopy, Elsevier, 2nd edition, **1984**, 2.
[30] SK Bharti; G Nath; R Tilak; SK Singh. *Eur J Med Chem*. **2010**, 45(2), 651.
[31] ZH Chohan; SH Sumrra; MH Youssoufi; TB Hadda. *Eur J Med Chem*. **2010,** 45(7), 273.
[32] TI Kashar; AH El-Sehli. *J Chem Pharm Res*. **2013**, 5(11), 474-483.
[33] S Chandra; S Raizada; M Tyagi; A Gautam. *Bioinorg Chem Appl J*. **2007**.
[34] XU Dongfang; MA Shuzhi; DU Guangying; HE Qizhuang; S Dazhi. *J Rare Earth.* **2008**, 26(5), 643.
[35] N Zhang; Yu-hua Fan; Z Zhang; J Zuo; Peng-fei Zhang; Q Wang; S Liu; CF Bi. *Inorg Chem Comm*. **2012**, 22, 68.
[36] TI Kashar; M Abdel-Motaal; K Emran; NA Sukar. *Eur Sci J*. **2017**, 13(3), 1857-7431.